One Case of Shock-free Deceleration of a Supersonic Flow in a Constant Cross Section Area Channel

Dmitry E. Khazov[1] iD

Air flows with supersonic speeds are used in many cases, for example, as aircraft air intakes, wind tunnels, and energy separation devices. In many cases it is necessary to decelerate the flow to sonic speeds. Traditionally the deceleration realized through the shocks system, which leads to total pressure losses. The article considers the method of deceleration of supersonic flows using permeable surfaces. In this case, the deceleration process occurs without shocks and, therefore, with lower total pressure losses. We have considered the flow in a tube with permeable wall located behind a supersonic nozzle. One-dimensional and axisymmetric mathematical models of such a device are developed. The calculation results are compared with experimental data. It is shown that, depending on the ratio of pressure inside the tube and the ambient pressure, different flow regimes inside the tube are possible: pure subsonic, transitional from supersonic to subsonic, and pure supersonic. The transition from supersonic to subsonic flow occurs without shocks due to the suction and friction combined effects.

Keywords: supersonic flow, permeable wall, Mach number, deceleration, injection/suction.

Introduction

The problem of a viscous supersonic flow deceleration in channels is of interest to researchers and engineers due to the importance of this problem for modern and future jet engines and wind tunnels. In the case of a constant cross section channel with impermeable walls, the supersonic flow is decelerated through a complex shocks structure and near-wall separation regions, generally called a pseudo-shock [4]. The deceleration of supersonic flow in the shock waves leads to the additional total pressure losses. Considerable potential in this regard has the use of permeable surfaces.

In the work [3], permeable (perforated) boundaries were used to accelerate the flow from sonic to supersonic speeds, as well as to equalize the non-uniformity of the supersonic flow. The authors of the paper [11] performed an experimental study of the flow in a permeable tube of constant cross section, installed in a supersonic nozzle. Experiments have shown that a transition from subsonic to supersonic flow occurs inside the tube.

As it can be seen from the works cited above, the use of permeable surfaces demonstrates the possibility of supersonic flow control. The purpose of this work is to study the processes of a supersonic flow deceleration in a channel of constant cross section with a permeable wall. To achieve this goal, it is necessary to develop numerical models that describe supersonic flows (with the possibility of passing through the critical point) in a channel of constant cross section with a permeable wall. Validate these models on the available experimental data, as well as perform a parametric study.

The article is organized as follows. Section 1 is devoted to the problem statement. In Section 2, we described two numerical models. The Section 3 discusses the main results of this study. The Conclusion summarizes the results of the study and indicates directions for further work.

---

[1]Institute of Mechanics, Lomonosov Moscow State University, Moscow, Russian Federation

1. Problem Statement

Let us consider the flow of a perfect gas in a channel of constant cross section with mass suction and friction. This type of flow can be found in transpiration cooling devices, fuel supply channels in burners, etc. In general, the device consists of a nozzle and a working channel with permeable wall. The permeable wall can be made of perforated or porous, permeable material. The parameters of porous materials, such as porosity and particle size, provide a different surface mass flux for the same pressure drop.

This article considers a device consisting of a supersonic nozzle and a cylindrical channel of constant cross section with a permeable wall (see Fig. 1). The gas accelerates to supersonic speeds in the nozzle and then enters the channel, where the flow decelerated. Since the wall is a permeable the pressure ratio in the channel p_{inn} and the ambient pressure p_{amb} will determine the direction of the flow through the wall: by $p_{inn} > p_{amb}$ gas will be sucked out from the channel; by $p_{inn} < p_{amb}$ gas will be injected into the channel. Thus, depending on the pressure drop inside the channel and the ambient pressure, various flow regimes can be realized.
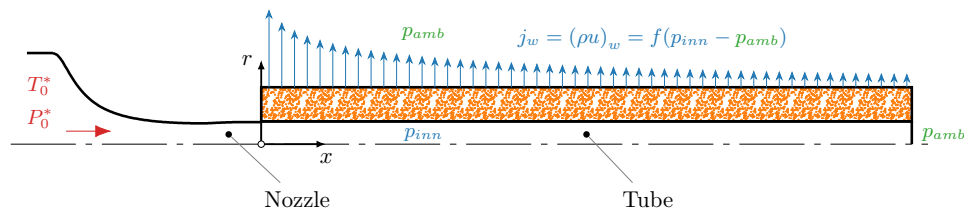

Figure 1. A sketch of the considered device

2. Numerical Models

We used one- and two-dimensional (axisymmetric) mathematical models for a detailed study of the processes occurring in the channel with permeable wall. The one-dimensional model allows to obtain the distribution of the main parameters (velocity, pressure, temperature, etc.) along the channel. It is assumed that all parameters are uniformly distributed across the section. In turn, the two-dimensional model allows to get more detailed information about the processes taking place inside the device. However, the use of such models is much more time consuming, as for the stage of model creation, and at the stage of a solution.

2.1. One-Dimensional Model

We used the well-known Shapiro–Hawthorne method [1] for a one-dimensional gas flow model. The main idea of the method is that the differential of each variable (velocity, pressure, temperature, etc.) is expressed through a linear combination of independent elementary factors of influence (such as friction, area change, external heat exchange, etc.); the coefficients of these linear combinations, called "influence coefficients", are expressed as functions of one variable (Mach number).

Based on the balance relations for the selected elementary volume and using the equation of state (perfect gas), we can obtain the following equation for the Mach number changing in a

constant area channel with friction, heat and mass transfer:

$$\frac{d\mathrm{M}^2}{\mathrm{M}^2} = \overbrace{\frac{1+k\mathrm{M}^2}{1-\mathrm{M}^2}\frac{dQ_w}{mc_pT}}^{\text{heat transfer}} + \overbrace{\frac{k\mathrm{M}^2\left(1+\frac{k-1}{2}\mathrm{M}^2\right)}{1-\mathrm{M}^2}4c_f\frac{dx}{d_h}}^{\text{friction}} + \overbrace{\frac{2\left(1+k\mathrm{M}^2\right)\left(1+\frac{k-1}{2}\mathrm{M}^2\right)}{1-\mathrm{M}^2}\frac{dm}{m}}^{\text{injection/suction}}, \quad (1)$$

where m is the mass flow rate, c_p is the specific heat at constant pressure, T is the thermodynamic temperature, Q_w is the net heat flow, c_f is the friction coefficient and d_h is the hydraulic diameter of the channel.

Equations for other variables (pressure, temperature, etc.) can be found in [1].

The amount of the heat (removed or added to the main flow) was determined from the following relation:

$$dQ_w = 4q_w\frac{A}{d_h}dx, \quad q_w = j_wc_p\left(T_{aw} - T^*\right), \quad (2)$$

where A is the cross-sectional area, $j_w = (\rho u)_w$ is the mass flux through permeable wall, T_{aw} is the adiabatic wall temperature and T^* is the stagnation temperature of the flow.

The value of mass flux j_w was determined from the Darcy–Forchhämer law for a cylindrical tube with inner and outer diameters d_{inn} and d_{out}, respectively [7]:

$$\frac{p_{amb}^2 - p_{inn}^2}{\mathrm{R}T\Delta d} = \alpha\mu\frac{d_{inn}}{\Delta d}\ln\frac{d_{out}}{d_{inn}}j_w + \beta\frac{d_{inn}}{d_{out}}j_w^2, \quad (3)$$

where p_{inn} is the pressure at the inner surface of a wall, $\Delta d = d_{out} - d_{inn}$ is the diameter difference, μ is the molecular viscosity and R is the specific gas constant.

Let us assume that a porous tube consists of uniform spherical particles of diameter d_p. In this case, values of viscous α and inertial β coefficients can be obtained from [7]:

$$\alpha = \frac{171\left(1-\varepsilon\right)^2}{\varepsilon^3 d_p^2}, \qquad \beta = \frac{0.635\left(1-\varepsilon\right)}{\varepsilon^{4.72}d_p}. \quad (4)$$

Values of porosity ε and diameter of spherical particles d_p determined based on the experimental flow characteristic of the sample of a permeable wall given in [12] which was used in present experiments and were as follows:

$$\varepsilon \approx 34\% \qquad d_p = 70 \times 10^{-6}\ \mathrm{m}. \quad (5)$$

The friction coefficient was determined from the Colebrook–White ratio [9]:

$$\frac{1}{\sqrt{\lambda}} = -2\log_{10}\left(\frac{2.51}{\mathrm{Re}\sqrt{\lambda}} + \frac{\Delta_s}{3.7}\right), \quad c_{f0} = \frac{\lambda}{4}, \quad (6)$$

where λ is the Darcy friction factor, $\Delta_s = h_s/d_h$ is the relative roughness. The Reynolds number is defined as $\mathrm{Re} = \rho u d_h/\mu$ with ρ the fluid density, d_h the hydraulic channel diameter, u the mass-mean fluid velocity and μ the fluid viscosity.

There is a need to take into account the effects of compressibility Ψ_M and injection/suction Ψ_b on the friction coefficient according to [6]:

$$c_f = \Psi_\Sigma c_{f0}, \quad \Psi_\Sigma = \Psi_\mathrm{M}\Psi_b, \quad (7)$$

$$\Psi_\mathrm{M} = \left(\frac{\arctan\mathrm{M}\sqrt{r\frac{k-1}{2}}}{\mathrm{M}\sqrt{r\frac{k-1}{2}}}\right)^2, \quad \Psi_b = \left(1 - \frac{b}{b_{cr}}\right)^2, \quad b_{cr} = 4, \quad (8)$$

where permeability parameter b was obtained by following:

$$b = \frac{\bar{\bar{j}}_w}{c_{f0}/2}, \quad \bar{j}_w = \frac{j_w}{(\rho u)_\infty}. \tag{9}$$

Massflow change was obtained from following relation:

$$dm = j_w d_h \pi dx. \tag{10}$$

Thus, using Eq. (1) (and others for pressure, temperature, etc.) and the closing relations Eqs. (2)–(10), it is possible to form a closed system of equations describing the flow in a channel with friction, heat transfer and injection/suction through a permeable wall. The system can be numerically integrated under the appropriate initial conditions:

$$\mathrm{M} = \mathrm{M}_0, \ u = u_0, \ T = T_0, \ p = p_0 \quad \text{at} \quad x = 0. \tag{11}$$

2.2. Two-Dimensional Model

The problem was modeled in the axisymmetrical formulation by using of ANSYS Fluent. Structured mesh was created by gmsh [2] preprocessor. The mesh size was about 10^5 cells. The discretization of the Reynolds-averaged Navier–Stokes equations (RANS), the energy equations and the equations of the corresponding turbulence model was performed on the basis of the control volume method. The second order upwind scheme was used for the spatial discretization. Based on previous study [5] the standard $k - \omega$ turbulence model was used.

The permeable wall was not modeled explicitly. The mass flux and heat flux were applied at the internal cylindrical surface of the porous tube. The value of mass flux was obtained on the basis of the Darcy–Forchhämer equation (3).

The following boundary conditions were used for the 2D model. Total pressure P_0^* and temperature T_0^* were specified at the inlet (see Fig. 1). The static pressure (p_{amb}) was specified at the outlet. The value of the specified static pressure is used only while the flow is subsonic. For the supersonic flow the pressure will be extrapolated from the flow in the interior.

3. Results and Discussion

We used two mathematical models developed above to simulate the flow in the experimentally investigated device in [8]. The profiled axisymmetric supersonic nozzle was used. The divergent section was profiled by using the method of characteristics. The nominal Mach number determined from the area ratio of the throat ($d_{cr} = 3.2$ mm) and the exit section ($d_{ex} = 3.4$ mm) in the case of isentropic air expansion is $\mathrm{M}_{is} = 1.43$. The coordinates of the nozzle contour are given in [8]. The permeable tube was made of synthetic corundum, $L = 150$ mm in length, $d_{out} = 10.4$ mm in the outer diameter, $d_{inn} = 3.5$ mm in the inner diameter. Note that the experimentally investigated permeable tube's inner surface was treated as rough with $h_s = d_p/2 = 35 \times 10^{-6}$ m ($\Delta_s = 0.01$).

The inlet total temperature was equal $T_0^* = 295.6$ K for all cases. The ambient pressure was equal $p_{amb} = 0.1$ MPa.

We extracted mass mean values from the 2D model for comparison with experimental and 1D data. Then we provided the parametric study by using the validated 2D model.

Figure 2 shows distribution of main flow parameters along the channel by $P_0^* = 0.4$ MPa. In addition to measured data (symbols), calculation data (lines) are also shown. The correspondence
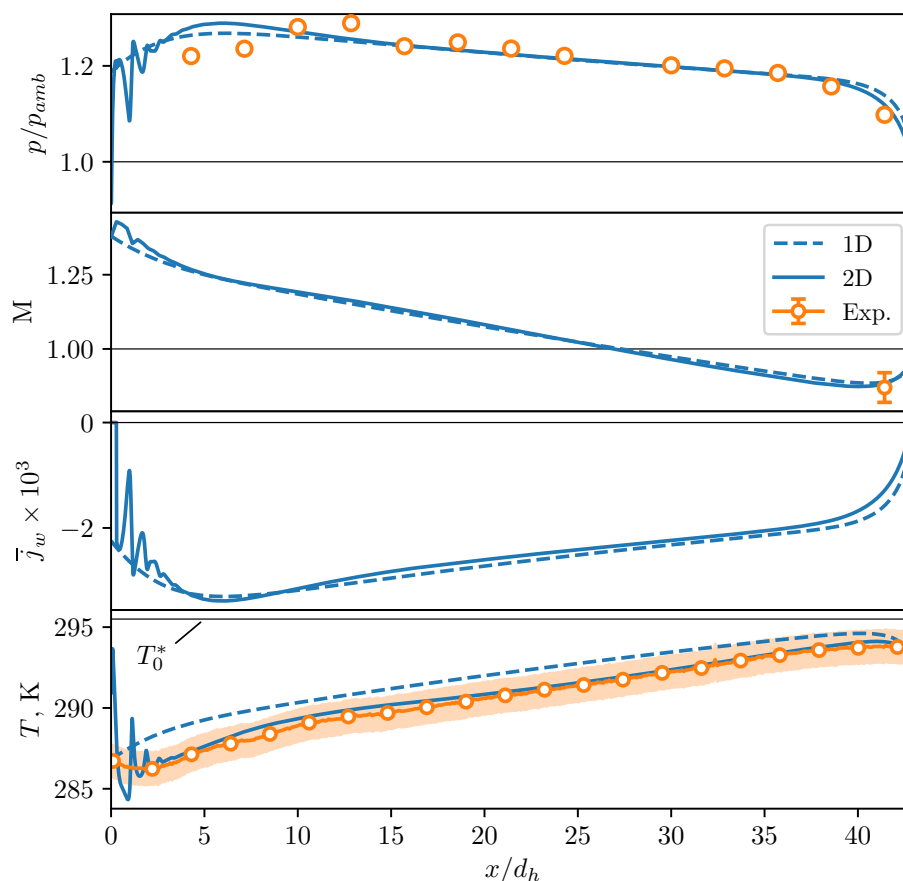
Figure 2. Main parameters distribution along the channel with a permeable wall. $P_0^* = 0.4$ MPa

between measured and calculated data is acceptable. The difference in temperature distribution is observed at the beginning of the channel ($x/d_h < 5$). It can be explained by the presence of shock waves generated by the backward step between nozzle and tube (see Fig. 3). As mentioned above, in the numerical model, the porous tube was not modeled explicitly. Therefore, the peaks of the wall temperature were observed. In contrast, in the experiment, the influence of shock waves on the wall temperature, as we assume, was smoothed by the porous tube thermal conductivity.
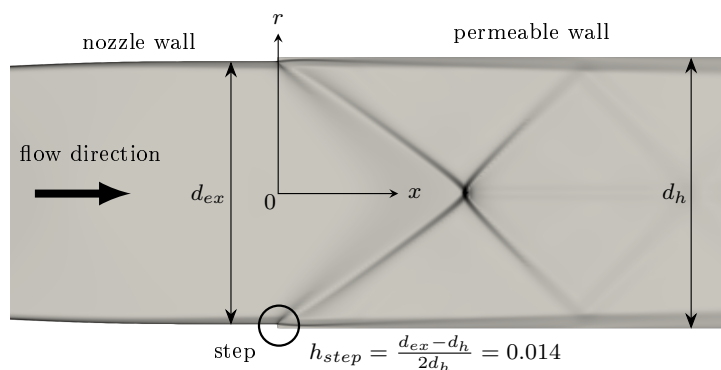

Figure 3. Numerical Schlieren of flow in the channel with a permeable wall. $P_0^* = 0.4$ MPa

The radial stagnation pressure distributions and static pressure at the wall were measured at $x/d_h = 41.4$ to obtain the Mach number distribution. Results of recovered Mach number

distributions are shown in Fig. 4. In addition to the measured values (symbols), the figure also shows the calculated data (lines). Mach number distribution along the channel with permeable wall is shown in Fig. 5.

From the Fig. 4 we can see that at lower initial stagnation pressures ($P_0^* < 0.5$ MPa) the flow is sub- or transonic at the section $x/d_h = 41.4$, although, for these pressures, the velocity at the nozzle exit is supersonic (see Fig. 5). This circumstance requires clarification.
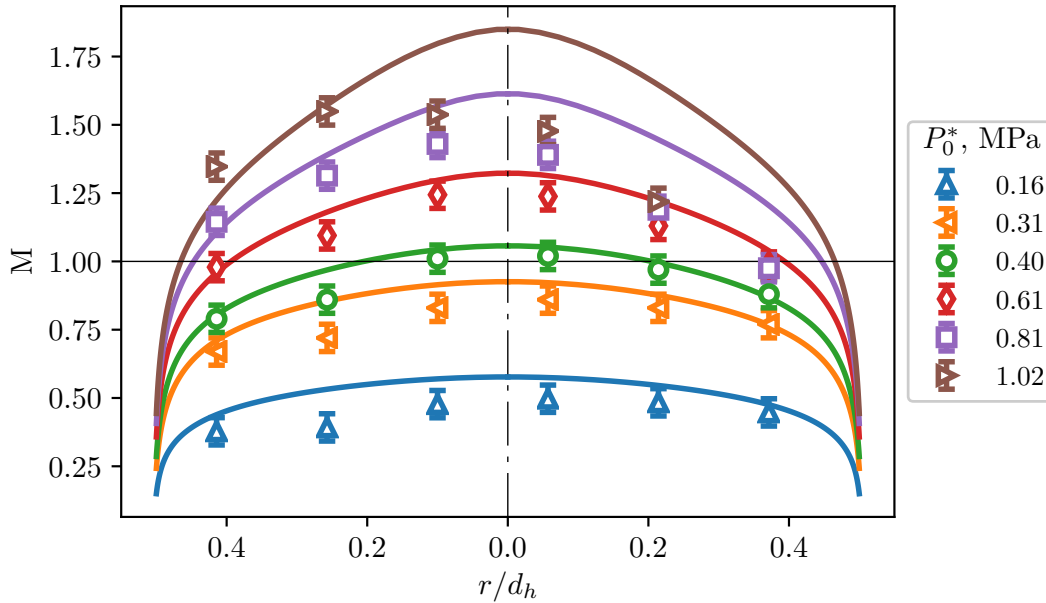

Figure 4. Mach number radial distribution at $x/d_h = 41.4$ by different initial stagnation pressure in plenum. Symbols are measured data; solid lines are results of 2D calculations

As it can be seen from the Fig. 2, throughout the entire length of the channel, the pressure exceeds atmospheric and, therefore, gas is sucked out along the whole length of the channel ($\bar{j}_w < 0$) through the permeable wall. The combination of the suction and friction leads to the fact that at a certain length ($x/d_h \approx 27$), the Mach number takes a critical value M = 1, and then the Mach number goes into the subsonic flow region. It should be noted that the transition, according to the calculation results, is not accompanied by shock waves, which can also be judged by the measured pressure distribution (see Fig. 2). As the pressure in the plenum increases, the critical section inside the channel (M = 1) shifts to the outlet section (see Fig. 5) and, starting from some value of $P_0^* > 0.5$ MPa, the flow throughout the whole length of the channel remains supersonic. The possibility of such passage through the sonic point will be discussed below.

Let us consider the physical possibility of the shock-free deceleration of a supersonic flow using a one-dimensional model. The Eq. (1) can be rewritten as it has been done in [10]:

$$\frac{1 - \mathrm{M}^2}{\mathrm{M}^2} \frac{d\mathrm{M}^2}{dx} = G(x), \tag{12}$$

where

$$
\begin{aligned}
G(x) = {} & \frac{1 + k\mathrm{M}^2}{mc_pT} \frac{dQ_w}{dx} + k\mathrm{M}^2 \left(1 + \frac{k-1}{2}\mathrm{M}^2\right) \frac{4c_f}{d_h} + \\
& + 2\left(1 + k\mathrm{M}^2\right)\left(1 + \frac{k-1}{2}\mathrm{M}^2\right)\frac{1}{m}\frac{dm}{dx} = \\
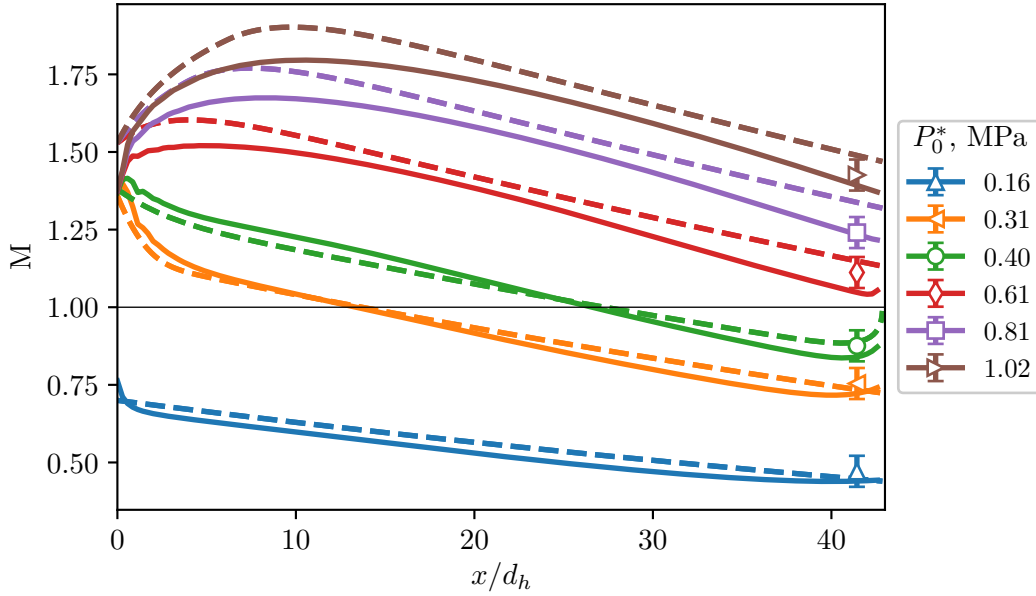& = G_Q + G_f + G_m,
\end{aligned} \tag{13}
$$

Figure 5. Mach number distribution along the channel with a permeable wall by different initial stagnation pressure in the plenum. Symbols are measured data; dashed lines are results of 1D calculations; solid lines are 2D calculations

where G_Q, G_f and G_m are elementary actions induced by heat transfer, friction and injection/suction, correspondingly.

Equation (12) shows that the local Mach number increases or decreases along the channel depending on the flow regime (subsonic or supersonic), as well as on whether the function G (summary action) is positive or negative, according to Tab. 1.

Table 1. Relations between G and $d\mathrm{M}^2/dx$ [10]

	$\mathrm{M} < 1$	$\mathrm{M} = 1$	$\mathrm{M} > 1$
$G < 0$	$-$	∞	$+$
$G = 0$	0	$0/0$	0
$G > 0$	$+$	∞	$-$

Therefore, the Mach number along the channel can vary in different ways, depending on whether the initial Mach number (M_0 at $x = 0$) is less or greater than one. Depending on whether the function G is always positive, negative, or changes sign. Figure 6 shows all the possible options.

As it is shown in the Fig. 6, the G function should change its value from positive to negative to implement the supersonic flow's deceleration to subsonic speeds (see Fig. 6e).

Figure 7 shows the changing of the Mach number and components of the function (see Eq. (13)) $\overline{G} = G/G(0)$ (normalized to initial value) along the channel for $P_0^* = 0.4$ MPa. As it can be seen from Fig. 7, the main factors are the mass removal $\overline{G}_m$ and the friction $\overline{G}_f$ (and they have different signs $\overline{G}_m < 0$ and $\overline{G}_f > 0$) along the whole channel length. At the initial section $\overline{G}_f > |\overline{G}_m|$ and $\overline{G} > 0$. Further, downstream the amount of sucked air decreases (see Fig. 2) and $\overline{G}_f$ also decreases (in absolute value). At the section $x/d_h \approx 27$ the value of the function is $\overline{G} = 0$ and Mach number takes the critical value $\mathrm{M} = 1$ according to Eq. (12).
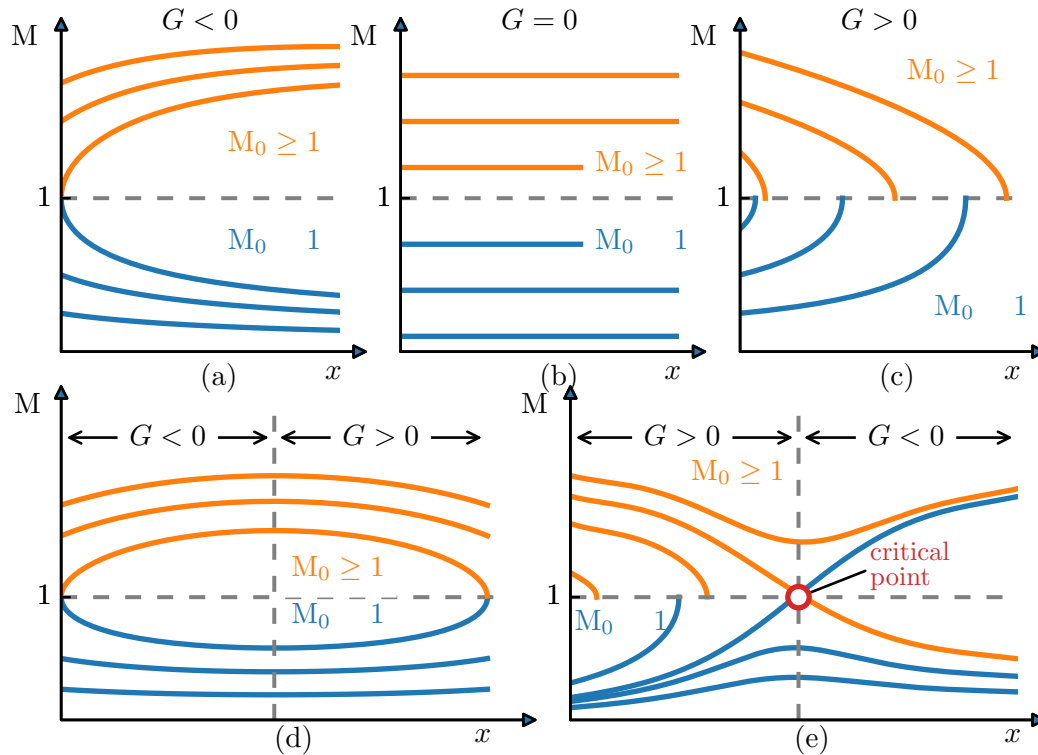
Figure 6. Possible options for changing the Mach number along a channel depending on the initial Mach number M_0 and the summary action G [10]

Summary action $\overline{G}$ changes its sign from positive to negative when passing through the critical section ($M = 1$).

Thus, the performed analysis shows that the shock-free deceleration in a constant cross-section channel with friction and suction through the permeable wall is possible. Moreover, the measured static pressure distribution (Fig. 2) and Mach number value at $x/d_h = 41.4$ (Fig. 4) confirm this conclusion.

It is possible to change the critical point location by using a tube with the different inner surface roughness. Figure 8 shows the local Mach number distribution (2D results) for different values of relative roughness. As it can be seen from the figure, a critical point locates upstream (closer to the initial section) for the bigger values of roughness. Then, as the roughness value decreases, the critical point shifts downstream. It can be noted that for the hydrodynamically smooth wall ($\Delta_s = 0$), there is no critical point and the pure supersonic flow is realized along the full channel length.

Conclusion

The flow in a supersonic nozzle with a permeable tube is considered. Two numerical models (one- and two-dimensional) have been developed that describe the processes occurring in such a device. The developed numerical models were validated against available experimental data. The experimental and calculated values are compared both along the channel axis and depending on the radius.

The presented results of numerical simulation of the flow in a permeable tube make it possible to conclude that a shock-free deceleration from supersonic to subsonic flow in a channel
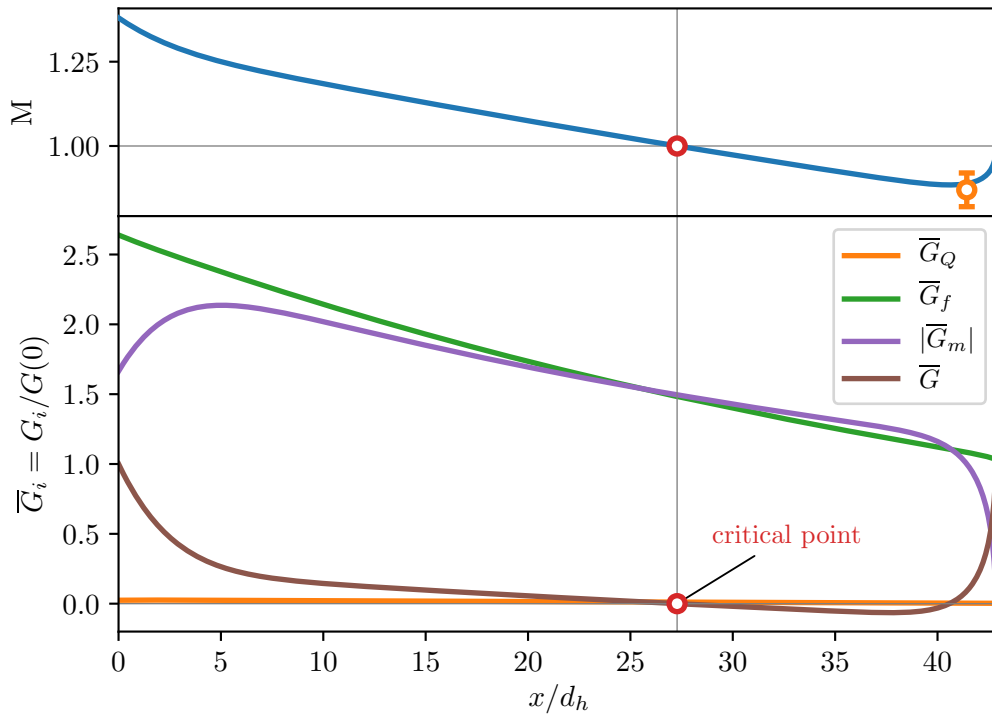
Figure 7. Changing of the Mach number and components of the function $\overline{G}$ along the channel with permeable wall. $P_0^* = 0.4$ MPa. Note, that for the presented case $\overline{G}_m$ is negative
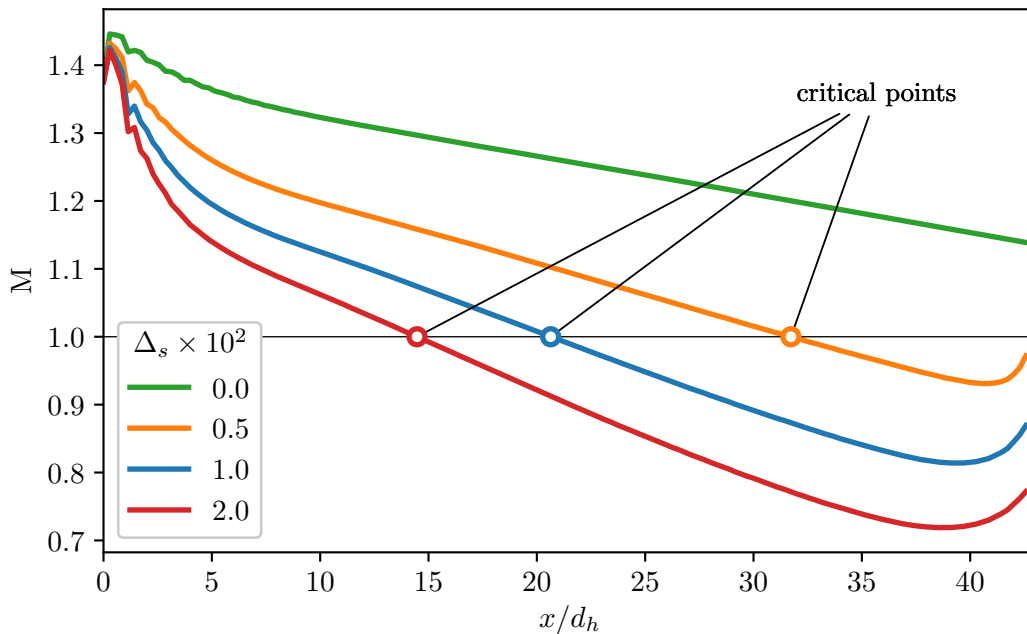

Figure 8. Influence of relative roughness on critical point location. $P_0^* = 0.4$ MPa

with permeable walls is possible. It is shown that the position of the transition (critical) point is determined by the pressure in the plenum and the relative roughness value. The comparison of the results of one-dimensional and two-dimensional models allows to conclude that the one-dimensional model is applicable to the analysis of such class of flows.

Acknowledgements

References

1. Emmons, H.: Fundamentals of gas dynamics. High Speed Aerodynamics and Jet Propulsion, Princeton University Press (1958)

2. Geuzaine, C., Remacle, J.F.: Gmsh: A 3-D finite element mesh generator with built-in pre- and post-processing facilities. International Journal for Numerical Methods in Engineering 79(11), 1309–1331 (Sep 2009). `https://doi.org/10.1002/nme.2579`

3. Grodzovskii, G., Nikol'skii, A., Svishchev, G., Taganov, G.: Supersonic gas flows in perforated boundaries. Mashinostroenie (1967)

4. Gus'kov, O.V., Kopchenov, V.I., Lipatov, I.I., *et al.*: Stagnation processes of supersonic flows in channels. Fizmatlit (2008)

5. Khazov, D.E.: On the question of gas-dynamic temperature stratification device optimization. Journal of Physics: Conference Series 891(1), 012078 (2017). `https://doi.org/10.1088/1742-6596/891/1/012078`

6. Kutateladze, S.S., Leontiev, A.I.: Turbulent Boundary Layers in Compressible Gases. Academic Press and Arnold (1964), (translated and exquisitely commented by D.B. Spalding)

7. Leontiev, A.I., Volchkov, E.P., Lebedev, V.P.: Thermal protection of plasmatron walls. Low temperature plasma, vol. 15. In-t teplofiziki SO RAN, Novosibirsk (1995)

8. Leontiev, A.I., Zditovets, A.G., Kiselev, N.A., *et al.*: Experimental investigation of energy (temperature) separation of a high-velocity air flow in a cylindrical channel with a permeable wall. Experimental Thermal and Fluid Science 105, 206–215 (2019). `https://doi.org/10.1016/j.expthermflusci.2019.04.002`

9. Rennels, D., Hudson, H.: Pipe Flow: A Practical and Comprehensive Guide. Wiley (2012)

10. Shapiro, A., H.: The dynamics and thermodynamics of compressible fluid flow, vol. 1. The Ronald Press Company (1953)

11. Vinogradov, Y., Leontev, A.: Gas flow in a supersonic axisymmetric nozzle with a permeable insert. Fluid Dynamics (5), 205–208 (1999)

12. Zditovets, A.G., Leontiev, A.I., Kiselev, N.A., *et al.*: Experimental study of the temperature separation of the air flow in a cylindrical channel with permeable walls. In: Proceedings of the 16th International Heat Transfer Conference, IHTC-16, Beijing, China (2018). `https://doi.org/10.1615/IHTC16.her.021878`